Bioorganic & Medicinal Chemistry 20 (2012) 2587–2594

Contents lists available at SciVerse ScienceDirect

Bioorganic & Medicinal Chemistry

journal homepage: www.elsevier.com/locate/bmc

Identification of benzoylisoquinolines as potential anti-Chagas agents

Kendall G. Byler [a], Marco Brito-Arias [b,*], Adrian Marquez-Navarro [c], Benjamin Nogueda-Torres [c], Luis G. Torres-Bustillos [b], Karina Martínez-Mayorga [a,*]

[a] Torrey Pines Institute for Molecular Studies, 11350 SW Village Parkway, Port St. Lucie, FL 34987, USA
[b] Unidad Profesional Interdisciplinaria de Biotecnología, Instituto Politécnico Nacional, Av. Acueducto s/n Colonia La Laguna Ticoman, Mexico, 07340 DF, Mexico
[c] Escuela Nacional de Ciencias Biológicas, Carpio y Plan de Ayala Colonia Santo Tomás, Mexico, DF 11340, Mexico

ARTICLE INFO

Article history:
Received 16 December 2011
Revised 14 February 2012
Accepted 20 February 2012
Available online 3 March 2012

Keywords:
Benzoyl isoquinolones
Trypanosoma cruzi
Chemical space
Structural similarity

ABSTRACT

A set of three 3-benzoyl substituted isoquinolones was synthesized in good yields and assayed for in vitro trypanocidal activity against *Trypanosoma cruzi*, the protozoan parasite that causes Chagas' disease. Depending on the concentration evaluated, a greater or equivalent reduction in the number of blood-borne trypomastigotes compared to that observed with benznidazole, a drug currently used to attack the parasite, was observed for two of the samples. In order to assess the potential of the 3-benzoylisoquinolone nucleus as a possible scaffold in the design of novel anti-trypanosomal lead structures, a computational analysis was performed using structural and inhibition information from both functional and target assays archived in the online database, ChEMBL. Chemical space projection of the synthesized compounds along with 3067 structures with known activities against *T. cruzi* shows that the isoquinolones occupy a sparsely-populated region of chemical space, indicating their potential for development as a novel class of trypanocidals. In addition, 2D and 3D structural similarity analyses revealed micromolar and submicromolar inhibitors of *T. cruzi* in ChEMBL with high similarity to the synthesized structures.

1. Introduction

Parasitic infections continue to be societal and health burdens, affecting millions of people, mainly in developing countries. Protozoal diseases such as leishmaniasis, malaria, sleeping sickness, and Chagas' disease assault populations in tropical and subtropical regions of Latin America, Africa, and Asia, where these diseases are endemic. The elevated cost of treatment of these diseases contributes to high mortality rates associated with infections in the world's most economically-disadvantaged areas. The high toxicity and cost associated with current treatments, along with a lack of efficacy during the chronic phase of the disease and emerging resistance to available therapy, highlight the need for the development of new antiparasitic drugs. It is important to note that remarkable initiatives,[1,2] have emerged around the world. American trypanosomiasis, or Chagas' disease,[3] is caused by the hemoflagellate protozoan *Trypanosoma cruzi*. It is estimated that 10–20 million people in Latin America are currently infected, with 25–90 million at risk of acquiring the parasite.[4,5] Available treatment for American trypanosomiasis is presently limited to two drugs: the nitro imidazole benznidazole and the nitrofuran nifurtimox (Fig. 1).

Although effective in the acute, short-term phase of the disease, nifurtimox (Nfx) and benznidazole (Bnz) are not effective in the more problematic chronic stage. Moreover, these two drugs are mutagenic and carcinogenic as well as significantly toxic, producing a variety of disturbing side effects. Both compounds are prodrugs that require conversion to the active component in the parasite; the mechanism of Nfx activity involves a reductive metabolite that produces toxic free radicals.[6] In the search for alternative approaches to combat this disease, new therapeutic targets have been identified and validated.[6] For *Trypanosoma cruzi*, recently identified biological targets include, but is not limited to: farnesyl pyrophosphate synthase (FPPS), *trans*-sialidase (TS), cruzain, trypanothione reductase (TR), glucose-6-phosphate dehydrogenase (GPDH), glyceraldehyde-3-phosphate dehydrogenase (GAPDH), and α-hydroxyacid dehydrogenase (HDH) and a number of compounds have been examined for their ability to inhibit these enzymes. Among them, 2,3-dihydro-3-deoxy-*N*-acetylneuraminic acid (DANA) has been crystallized with *T. cruzi* trans-sialidase[7] and phenothiazine derivatives have been assayed for *T. cruzi* trypanothione reductase activity.[8]

Alternatively, a convenient option currently employed in many drug discovery efforts involves repurposing drugs marketed for the treatment of other conditions. In the search for anti-Chagas agents; risedronate,[9] camptothecin,[10] and allopurinol[11] have been shown to inhibit the progression of the disease (Fig. 1).

The efficacy of 2-substituted quinolines found in medicinal plants against *Leishmania* spp.[12,13] and *T. cruzi*[14] has motivated

* Corresponding authors.
E-mail address: kmartinez@tpims.org (K. Martínez-Mayorga).

0968-0896/$ - see front matter © 2012 Elsevier Ltd. All rights reserved.
doi:10.1016/j.bmc.2012.02.046

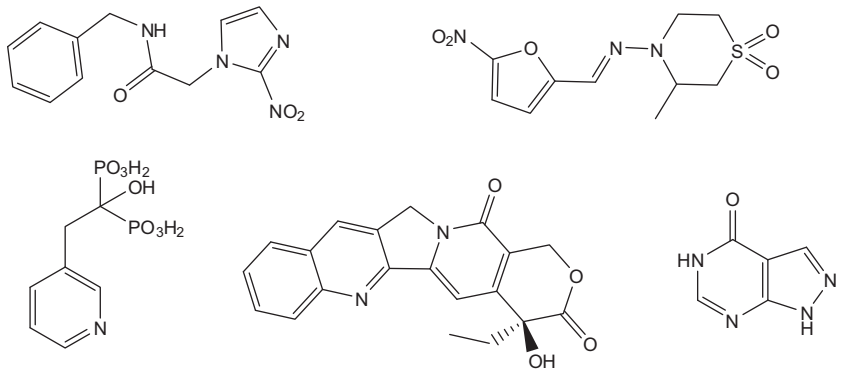

Figure 1. Anti-Chagas drugs benznidazole and nifurtimox and approved drugs with recently reported activity in *T. cruzi* (*l to r*): risedronate, camptothecin and allopurinol.

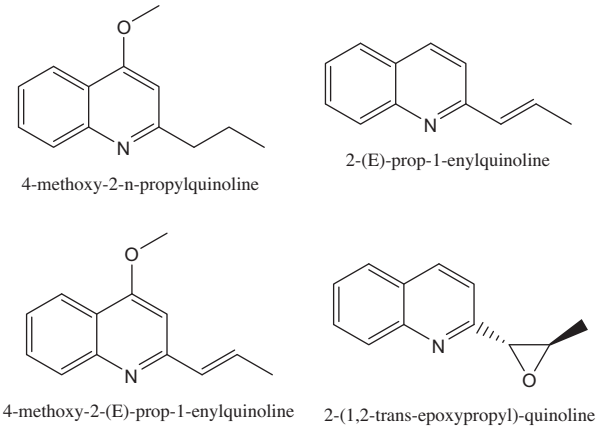

Figure 2. Drugs with known activity against enzymatic targets in *Trypanosoma cruzi*.

the exploration of quinolines as privileged scaffolds against parasitic diseases and viral infections. Synthetic quinolines obtained and assayed by Fakhfakh, et al. showed promising in vitro activity[15] against leishmania/HIV co-infections. Although these compounds were less active than the reference compound, suramin, they represent new lead molecules for further optimization (Fig. 2). Related chemical structures, also explored as anti-leishmania agents, are naphthylisoquinoline alkaloids. Ponte-Sucre, et al. showed that naphthylisoquinoline alkaloids and synthetic analogs are effective against intracellular amastigotes in the submicromolar range.[16]

Public domain repositories of bioactive compounds[17] and associated data provide a valuable means of collecting and sharing information, performing data mining, and avoiding duplicated efforts—ultimately aiding in the discovery of new medications. Examples of such sources are the ChEMBL database,[18] PubChem Central[19,20] and BindingDB.[21] Retrieval of chemical structures along with antiparasitic activity data reported in the literature can be obtained from the ChEMBL website (https://www.ebi.ac.uk/chembl) and is freely available for analysis.

In this work, we present the analysis of the structural and physicochemical properties of compounds tested against *T. cruzi* in enzymatic and functional assays reported in the ChEMBL database. 3-benzoylisoquinolones were synthesized and evaluated for their ability to reduce the number of live parasites in infected blood. The reaction scheme involves the Gabriel-Colman rearrangement,[22] and subsequent electrophilic aromatic substitution at position 3 of the benzoyl ring. The structural and physicochemical properties of 3-benzoylisoquinolones were analyzed in relation to those reported in the literature and extracted from the ChEMBL database.

2. Results and discussion

2.1. Synthesis of benzoylisoquinolones

The synthesis of benzoylisoquinolone derivatives **4a–c** was carried out according to Scheme 1, starting from the condensation reaction between potassium phthalimide **1** and 2-bromacetophenone **2** in DMF at room temperature to provide **3** in good yields. The next step involved the reaction of compound **3** with sodium methoxide solution under reflux to provide benzoyl isoquinolone **4a**. The formation of this heterocycle proceeded via the Gabriel-Colman rearrangement and its characterization was achieved by X-ray diffraction.[23] Modification of the benzoyl isoquinolone nucleus at position 3 was performed under standard conditions to provide the nitro derivative **4b**, followed by reduction under catalytic hydrogenation to yield the amino derivative **4c** in quantitative yields.

2.2. Trypanocidal activity of benzoylisoquinolones

Assays for trypanocidal activity of the isoquinolones were carried out at the three concentrations described below, including the drug benznidazole as a reference standard. The efficacy of compound **4b** was observed to increase at a high concentration (161 μM), reaching a maximum trypanocidal activity of 47% after 24 h incubation. Compound **4c** exhibited greater trypanocidal activity compared to that observed for Bnz at concentrations of 18 and 36 μM, although there was a decrease in activity relative to both Bnz and **4b** at 178 μM (Fig. 3). In addition to eliciting a decrease in the number of live bloodstream parasites, the motility of the remaining parasites was markedly reduced upon introduction of Bnz. The parasites treated with **4c** also exhibited the weak motility observed in the parasites treated with Bnz. Compound **4a** elicited no decrease in the number of bloodstream parasites at any concentration.

2.3. Physicochemical properties of compounds evaluated against *T. cruzi*

A total of 3067 compounds with reported activity data from inhibition assays against specific enzymes in *T. cruzi,* and against the whole organism in functional assays, were retrieved from the ChEMBL database. The ranges of activity values and the number of compounds per data set are summarized below in Table 1.

A principal component analysis (PCA) was carried out as described in the Section 4 using physicochemical descriptors calculated in MOE 2009.10[24] for the combined set of 3067 structures in order to examine the region of chemical space occupied by the benzoylisoquinolones in relation to structures screened against *T. cruzi*. To project the structures into a chemical space representa-

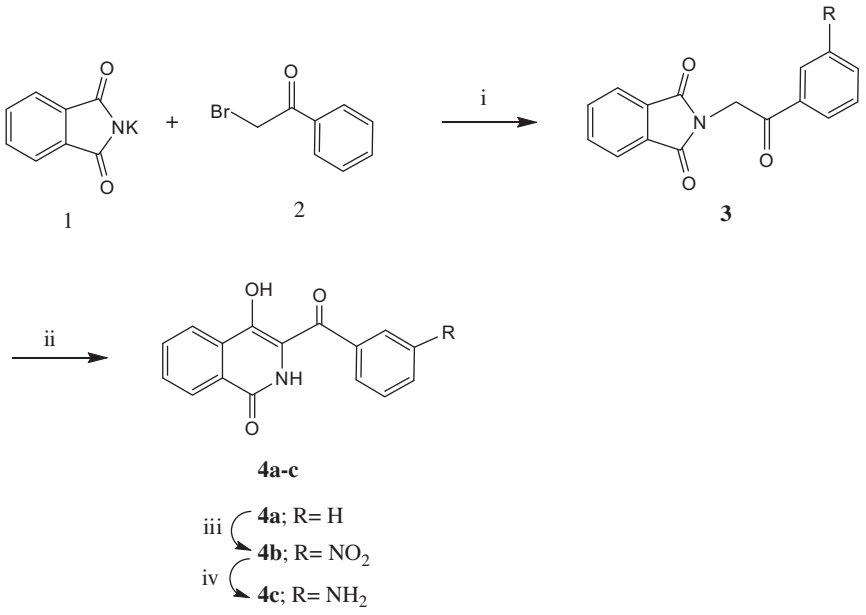

Scheme 1. Synthesis of benzoylisoquinolone derivatives.

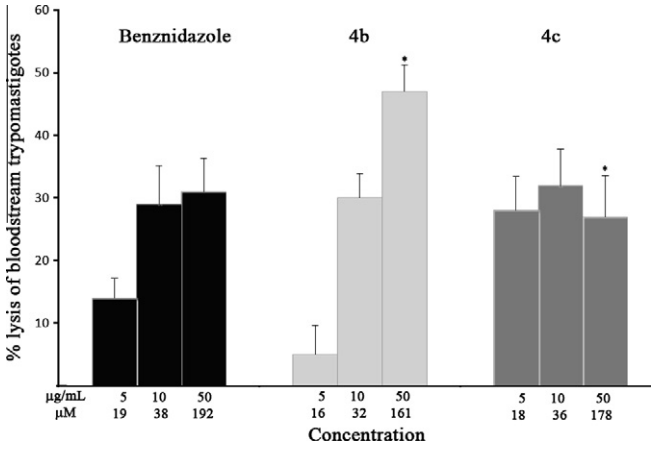

Figure 3. Anti-trypanosomal activity of compounds **4b-c** in *Trypanosoma cruzi* after 24 h of incubation at 4 °C. Statistical significance was determined at P <0.05.

tion that would reflect properties relevant to inhibitory activity, partial least squares (PLS) regressions of activity data were employed to evaluate the relative contribution of each descriptor to the prediction of activity in each data set and across all sets. The descriptors identified as having the highest correlations with activity across all data sets are shown in Figure 4, along with their contribution to each principal component (PC) as a percentage of normalized transform coefficients. Of the size and shape descriptors, radius of gyration contributes much more substantially to all activity models versus molecular weight, reflecting the large variance in the linear size of compounds tested in the inhibition assays. The prominence of the Kier flexibility index among the descriptors also reveals a significant variance in the flexibility of assayed compounds. The charge-based descriptors are featured much less prominently, owing to smaller variations in the charge distributions in the data sets when compared with those of the size and shape descriptors. Nevertheless, the polarizability descriptor, bpol, and the charge descriptors, ASA, ASA+, VSA_POS and VSA_P-POS, make consistent contributions to the PLS regressions and were included in a reduced set of ten descriptors that were then used in a second PCA to produce principal components for the activity-correlated chemical space projection.

The factor loadings of the principal components were used to identify the descriptors with significant contributions and these were used in the second PCA. The first three PC's, with a total explained variance of 80%, were then plotted as a three-dimensional activity-correlated chemical space into which all structures were projected, as shown in Figure 5. Details of the visualization of the chemical space and recent applications are reported elsewhere.[25,26]

The three benzoylisoquinolones appear as gray spheres near the periphery of the distribution, with the nitro-substituted structure,

Table 1
Structures from ChEMBL database used in the structural analysis with associated inhibition value ranges.

Assay	Reported inhibition	Range	Number of unique structures
Functional			
	IC_{50}	0.25nM – 17 mM	1895
	EC_{50}	4.0 nM–10 µM	318
	% inhibition	~	212
Target			
Cruzain	IC_{50}	0.1 nM–10 mM	403
Glyceraldehyde-3-phosphate dehydrogenase (GAPDH)	IC_{50}	100 nM–692 µM	16
Trypanothione reductase (TR)	IC_{50}	300 nM–133 µM	200
trans-Sialidase (TS)	IC_{50}	580 nM–1 mM	23

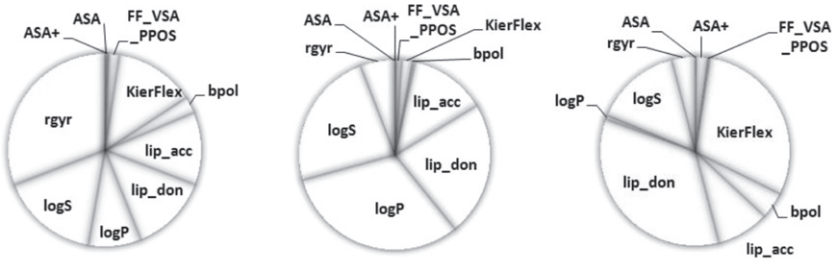

PC1	PC2	PC3	Descriptor	
0.3%	0.0%	0.1%	**ASA**	Water accessible surface area (1.4Å)
0.3%	0.1%	2.0%	**ASA+**	Water accessible surface area of all atoms with positive partial charge
1.8%	1.0%	0.4%	**FF_VSA_PPOS**	Total positive polar van der Waals surface area
13.4%	1.8%	29.8%	**KierFlex**	Kier molecular flexibility index
2.8%	0.5%	4.6%	**bpol**	Sum of the absolute value of the difference between atomic polarizabilities of all bonded atoms
12.2%	12.9%	9.0%	**lip_acc**	Number of O and N atoms
13.1%	22.8%	34.5%	**lip_don**	Number of OH and NH atoms
8.8%	31.6%	0.8%	**logP(o/w)**	Log of the octanol/water partition coefficient
16.4%	23.3%	14.7%	**logS**	Log of the aqueous solubility (mol/L)
30.8%	5.9%	4.0%	**rgyr**	Radius of gyration

Figure 4. Descriptor contributions to principal components used in the chemical space projection.

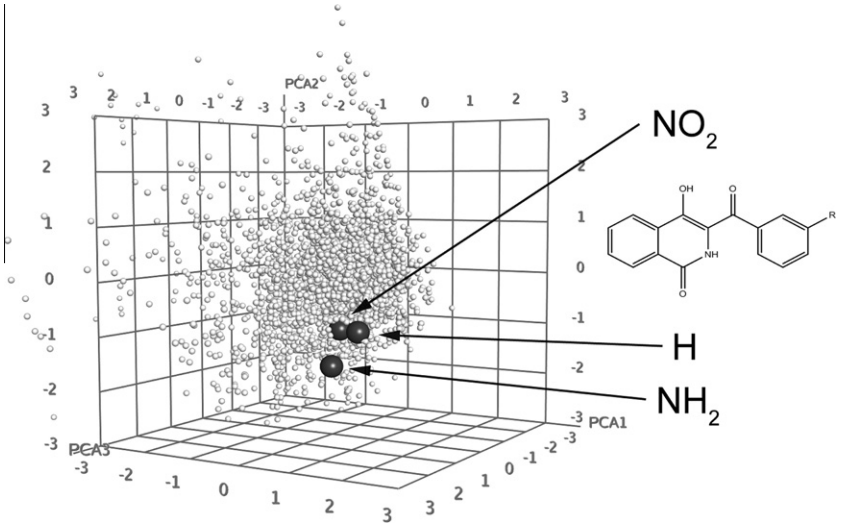

Figure 5. Principal component space projection of combined set of *T. cruzi* assay compounds from ChEMBL database with isoquinolone structures as large gray spheres.

4b, closest to the main group. The amino structure, **4c**, is the farthest outlier of the synthesized compounds, occupying a sparsely-populated region, suggestive of unexplored chemical space.

2.4. Structural comparison of benzoylisoquinolones with compounds evaluated against *T. Cruzi*

A structural similarity analysis of the benzoylisoquinolones was performed against each of the ChEMBL data sets using both 2D and 3D representations in order to identify structurally similar compounds with known activities in *T. cruzi*. We have previously reported the benefits of combining 2D and 3D structural representations.[27]

In the 3D analysis, twenty conformers of each isoquinolone structure were generated using OMEGA[28] and aligned to all (500 max.) conformations of each structure in the reference data using ROCS.[28] For large datasets a reduction in the number of conformers analyzed can be valuable. To that end, rmsd-based clustering followed by the selection of conformers based on a penalty function have shown useful.[29] ROCS uses molecular volumes represented by Gaussian functions to overlay structures, and returning the sum of the Tanimoto indices of 3D structure similarity and chemical feature similarity (TanimotoCombo score).[30,31] Further details of this method and applications can be found in the literature.[31–33]

For the 2D portion of the analysis, five molecular fingerprints (Atom Pairs, Radial, MACCS keys, TGD, and piDAPH3) were generated for each structure, and the Tanimoto index used to rank compounds most similar to the isoquinolones. The selection of these fingerprints as suitable representations for similarity searching has been described previously.[34,35] The structures with the highest Tanimoto scores for each fingerprint or ROCS alignment from the functional assays are presented in Table 2, along with

Table 2
Structures from ChEMBL functional sets identified as structurally similar to the benzoylisoquinolones

	4a	4b	4c
ROCS alignments	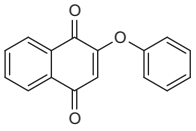 $T_s = 0.730$ IC50 = 1.26μM **CHEMBL256155**	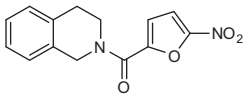 $T_s = 0.694$ EC50 = 42nM **CHEMBL1609301**	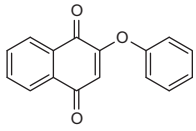 $T_s = 0.673$ IC50 = 1.26μM **CHEMBL256155**
Radial fingerprints	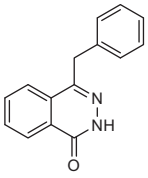 $T_s = 0.168$ $IC_{50} > 420\mu M$ **CHEMBL66761**	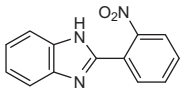 $T_s = 0.140$ IC50 = 117μM **CHEMBL209918**	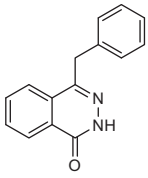 $T_s = 0.149$ $IC_{50} > 420\mu M$ **CHEMBL66761**
Atom Pairs fingerprints	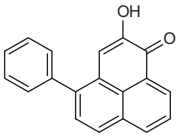 $T_s = 0.629$ $IC_{50} > 367\mu M$ **CHEMBL1164085**	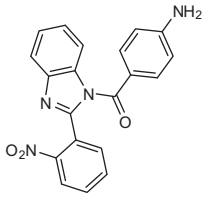 $T_s = 0.500$ $IC_{50} = 80\mu M$ **CHEMBL508548**	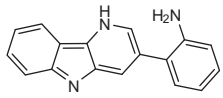 $T_s = 0.477$ $IC_{50} = 10.4\mu M$ **CHEMBL368103**
MACCS keys	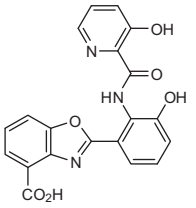 $T_s = 0.620$ 96% inhibition @ 12μM **CHEMBL463985**	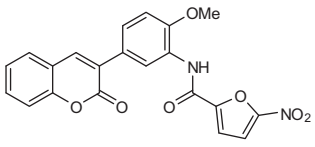 $T_s = 0.700$ $EC_{50} = 262nM$ **CHEMBL1335703**	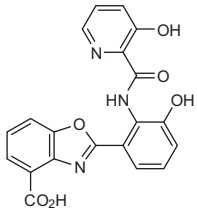 $T_s = 0.660$ 96% inhibition @ 12μM **CHEMBL463985**
TGD fingerprints	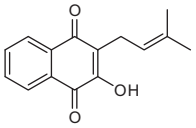 $T_s = 0.810$ $IC_{50} = 31.3\mu M$ **CHEMBL15193**	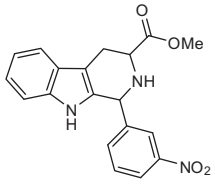 $T_s = 0.810$ $IC_{50} = 22.2\mu M$ **CHEMBL488544**	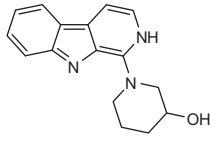 $T_s = 0.780$ $IC_{50} = 73\mu M$ **CHEMBL186474**
piDAPH3 fingerprints	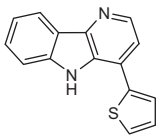 $T_s = 0.650$ $IC_{50} = 1.8\mu M$ **CHEMBL366482**	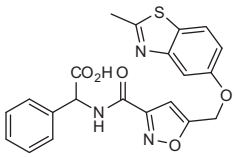 $T_s = 0.650$ $IC_{50} > 90\mu M$ **CHEMBL566122**	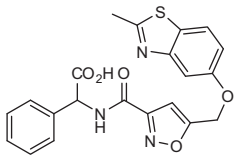 $T_s = 0.590$ $IC_{50} > 90\mu M$ **CHEMBL566122**

their ChEMBL identifiers and inhibition values, while those for the set of target assays are shown in Table 3.

Many of the structures identified as most similar to the isoquinolones by Tanimoto score in the target assays had scores slightly

Table 3
Structures from ChEMBL target sets identified as structurally similar to the benzoylisoquinolones.

	4a	4b	4c
ROCS alignments	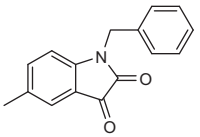 $T_s = 0.638$ cruzain IC_{50} >> 1μM **CHEMBL115581**	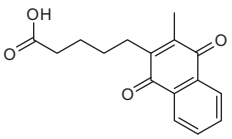 $T_s = 0.638$ TR IC_{50} > 50μM **CHEMBL134615**	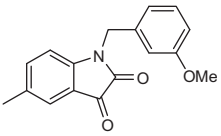 $T_s = 0.626$ cruzain IC_{50} = 2μM **CHEMBL324722**
Radial fingerprints	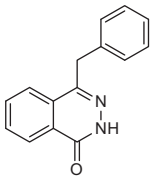 $T_s = 0.168$ cruzain IC_{50} > 100μg/mL **CHEMBL66761**	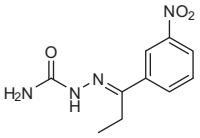 $T_s = 0.175$ cruzain IC_{50} = 860nM **CHEMBL373586**	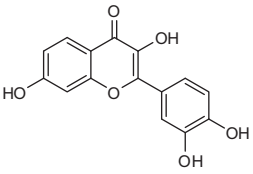 $T_s = 0.773$ cruzain IC_{50} > 60μM **CHEMBL31574**
Atom pairs fingerprints	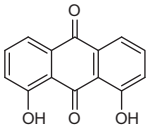 $T_s = 0.542$ TS IC_{50} = 710μM **CHEMBL53418**	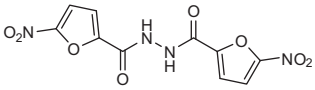 $T_s = 0.396$ TR IC_{50} > 50μM **CHEMBL118432**	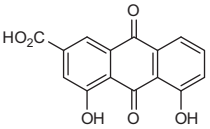 $T_s = 0.433$ TS IC_{50} = 14μM **CHEMBL418068**
MACCS Keys	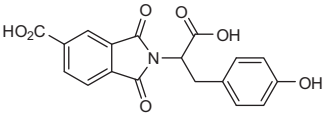 $T_s = 0.620$ cruzain IC_{50} > 10mM **CHEMBL258538**	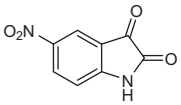 $T_s = 0.720$ cruzain IC_{50} >> 10μM **CHEMBL118305**	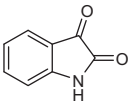 $T_s = 0.580$ cruzain IC_{50} >> 10μM **CHEMBL326294**
TGD fingerprints	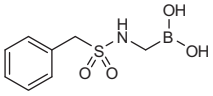 $T_s = 0.830$ cruzain IC_{50} > 500μM **CHEMBL1231476**	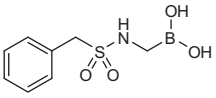 $T_s = 0.790$ cruzain IC_{50} > 500μM **CHEMBL1231476**	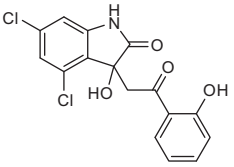 $T_s = 0.820$ cruzain IC_{50} = 73μM **CHEMBL259139**
piDAPH3 fingerprints	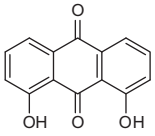 $T_s = 0.620$ TS IC_{50} = 710μM **CHEMBL53418**	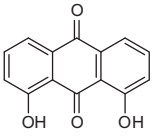 $T_s = 0.590$ TS IC_{50} = 710μM **CHEMBL53418**	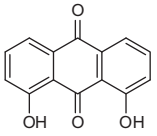 $T_s = 0.560$ TS IC_{50} = 710μM **CHEMBL53418**

lower than, but comparable to, those of the functional assays for all the fingerprints used, save for the radial fingerprints, which consistently yielded poor Tanimoto scores. The majority of similar structures in the target sets were obtained from the cruzain set, although the activity values for these compounds were rather poor in most cases, with inhibitory concentrations ranging from 1–10 μM. By comparison, the most similar structures in the functional inhibition assays had slightly higher similarity indices to the benzoylisoquinolones, with the best ROCS alignment for **4b**, a nitro-substituted isoquinoline compound (CHEMBL1609301), having a half maximal effective concentration of 42 nM, as determined by a cell-based luminescence high-throughput screen of amastigotes in NIH3T3 mouse fibroblasts. The most similar compound to the amino product, **4c**, using MACCS keys, was CHEMBL463985, with 96% inhibition (at 12 μM) of Tulahuen C2C4 amastigotes in L6 rat skeletal myoblasts.

The similarity matches from the target assays yielded only one micromolar inhibitor to **4c**, CHEMBL324722, an indoline dione with a reported IC_{50} value of 2 μM to cruzain. We observed no other low-concentration inhibitors in the matches from the target

sets; rather, the most similar structures had poor inhibition values. Therefore, based on this analysis, the specific target of interaction of the compound studied here cannot be suggested.

3. Conclusions

The present work illustrates the potential of the easily-synthesized 3-benzoyl-4-hydroxyisoquinolin-1(*2H*)-one scaffold as anti-Chagas agents. Two of the samples evaluated exhibited greater trypanocidal activity than the reference drug benznidazole at the assayed concentrations. Considering that nitro derivatives usually show different degrees of toxicity, further studies regarding potential side effects should be evaluated in the case of **4b**.

It is unclear from the structural similarity analysis the specific target with which the benzoylisoquinolones may be interacting to effect their trypanocidal action, as all but one structure with significant similarity have poor activities in their respective target inhibition assays.

The region occupied by the synthesized compounds in the property space projection lies at the outer edge of the distribution of compounds with known activity in *T. cruzi*. And in the case of **4c**, this region is also sparsely populated, suggesting that the isoquinolone scaffold represents an under-explored domain for trypanocidals, with possibilities for the discovery of novel active compounds.

This work leads to further explore the potential of benzoylisoquinolones as anti-Chagas agents; preparation of analogues and structure–activity relationships studies are warranted.

4. Methods

4.1. Synthesis of benzoylisoquinolones

The lack of purity of the compounds prevents us from unambiguously characterize the samples. However, our previously reported X-ray structure of compound **4a**,[23] synthesized in a similar manner, validates the synthetic method employed. Additional studies are under way to fully characterize the chemical structures and to prepare of analogues for SAR studies. The NMR spectra for **4b** and **4c** are provided as Supplementary data, as well as the crystallographic information for compound **4a**.[23]

4.2. In vitro trypanocidal assay

The NINOA strain of *T. cruzi* employed in this study was isolated from an acute case of Chagas' disease in the city of Oaxaca, Mexico. The live parasite was maintained in the laboratory in the triatomine vector *Meccus pallidipennis* (Insecta:Hemiptera) and in female white mice, *Mus musculus*.

All compounds were initially dissolved in dimethyl sulfoxide (DMSO) at a concentration of 10 mg/mL, followed by serial dilutions with distilled water to achieve the desired concentrations. All compounds were evaluated against trypomastigotes obtained by cardiac puncture of infected mice at the peak of parasitemia using benznidazole (Bnz) as a reference. Heparin was used as an anticoagulant. The infected blood was diluted with sterile 0.85% saline solution and the parasites were adjusted to 1×10^6 bloodstream trypomastigotes/mL. Bioassays were run in triplicate in 96-well plates containing 195 μL of the trypomastigote suspension and 5 μL of each compound at a concentration of 5, 10 and 50 μg/mL. A DMSO control was assayed in parallel, with the concentration of DMSO never exceeding 1%. The plates were incubated at 4 °C for 24 h, after which the trypomastigotes were counted using the method described by Brener.[36] Anti trypanosomal activity was expressed as a percentage of the reduction in the number of live parasites compared to the control (non-treated parasites).

4.2.1. Statistical analysis

All results were expressed as the mean percentage (%) of lysis of a triplicate. Data were analyzed using Dunnett's method to compare the treatment groups with the control. Statistical significance was determined as $P < 0.05$.

4.3. Computational methods

4.3.1. Data selection

An assay search of the ChEMBL database using the keywords *Trypanosoma cruzi* (CHEMBL368) yielded three major sets of assay data, which were downloaded 10/2011 as individual sets, according to the reported measure of inhibition. The compound data for the functional assays:% inhibition (212 unique structures from 62 assays), EC_{50} (318 unique structures from one assay, CHEMBL1614129), and IC_{50} (1895 unique structures from 171 assays) were converted to three-dimensional structures in MOE 2009.10 and minimized with the Merck '94 force field. In addition to the functional assays, compounds in ChEMBL used in specific target assays in *T. cruzi* were also downloaded and their structures prepared as previously described: [glyceraldehyde-3-phosphate dehydrogenase (GAPDH), CHEMBL5926, IC_{50} values (100 nM-629 μM), 16 unique structures from one assay, CHEMBL1023015]; [cruzain, CHEMBL3563, IC_{50} values (0.1 nM–10 mM), 403 unique structures from 29 assays]; [trypanothione reductase (TR), CHEMBL5131, IC_{50} (300 nM–133 μM), 200 unique structures from 16 assays]; [trans-sialidase (TS), CHEMBL5126, IC_{50} (580 nM–1 mM), 23 unique structures from 1 assay, CHEMBL1154902].

4.3.2. Principal Component Analysis

Twenty-four physicochemical descriptors (Supplementary Table S1) were calculated for all minimized structures in MOE 2009.10 and used in PC analysis. Partial least squares regressions of the PC's (as normalized composite descriptors) were performed using each set of target inhibition data, as well as for the functional inhibition data. The (descriptor) factor loadings of the three PC's with the largest PLS coefficients in each regression were averaged, weighting by the normalized PLS coefficient for each PC, and scaled to inspect the relative importance of each descriptor to the prediction of inhibition for each target. Since the functional assays reported different measures of activity, three separate regressions were performed as described and combined, weighting by the number of compounds in each set. Ten descriptors that contributed significantly to the regressions in each data set were selected for a second PCA, which was used in the chemical space projection.

4.3.3. Structural similarity

The 3D structural similarity analysis was performed using the OpenEye[28] programs. A maximum of 500 conformations for each structure in the 3D alignment analysis were generated using OMEGA 2.4.1 and each of the benzoylisoquinolone conformations were aligned to each of the conformations in each data set using ROCS 3.0.0 (MMFF94s force field), ranking alignments by TanimotoCombo score. The TanimotoCombo score was multiplied by ½ in order to compare similarities with other Tanimoto scores in the 2D analyses.

In the 2D structural similarity analysis, the *Atom Pairs* and *Radial* fingerprints were generated using Canvas 1.4.112[37] and the *TGD* and *piDAPH3* fingerprints, as well as the 166-bit MACCS keys were generated with MOE 2009.10.

Acknowledgments

MBA is grateful to SIP and COFAA IPN for financial support. KMM thanks the State of Florida, Executive Officer of the Governor's Office of Tourism, Trade and Economic Development for

funding. Authors thank OpenEye Scientific Software for providing the OMEGA, ROCS and VIDA programs.

Supplementary data

Supplementary data associated with this article can be found, in the online version, at doi:10.1016/j.bmc.2012.02.046.

References and notes

1. Chatelain, E.; Ioset, J. R. *Drug Des. Dev. Ther.* **2011**, *5*, 175.
2. Scott, W. L.; O'Donnell, M. J. *J. Comb. Chem.* **2009**, *11*, 3.
3. da Costa Santiago, H.; Tanowitz, H. B.; Weiss, L. M.; Montgomery, S. P. *PLoS Neglected Trop. Dis.* **2011**, *5*, e1136.
4. Lammie, P. J.; Hotez, P. J.; Bottazzi, M. E.; Franco-Paredes, C.; Ault, S. K.; Periago, M. R. *PLoS Neglected Trop. Dis.* **2008**, *2*, e300.
5. Reithinger, R.; Tarleton, R. L.; Urbina, J. A.; Kitron, U.; Gürtler, R. E. *Br. Med. J.* **2009**, 338.
6. Rivera, G.; Bocanegra-García, V.; Ordaz-Pichardo, C.; Nogueda-Torres, B.; Monge, A. *Curr. Med. Chem.* **2009**, *16*, 3286.
7. Buschiazzo, A.; Amaya, M. A. F.; Cremona, M. A. L.; Frasch, A. C.; Alzari, P. M. *Molecular Cell* **2002**, *10*, 757.
8. Chan, C.; Yin, H.; Garforth, J.; McKie, J. H.; Jaouhari, R.; Speers, P.; Douglas, K. T.; Rock, P. J.; Yardley, V.; Croft, S. L.; Fairlamb, A. H. *J. Med. Chem.* **1998**, *41*, 4910.
9. Bouzahzah, B.; Jelicks, L. A.; Morris, S. A.; Weiss, L. M.; Tanowitz, H. B. *Parasitol. Res.* **2005**, *96*, 184.
10. Bodley, A. L.; Shapiro, T. A. *Proc. Natl. Acad. Sci. U.S.A.* **1995**, *92*, 3726.
11. Gobbi, P.; LoPresti, M. S.; Fernández, A. R.; Enders, J. E.; Fretes, R.; Gea, S.; Paglini-Oliva, P. A.; Rivarola, H. W. *Parasitol. Res.* **2007**, *101*, 1459.
12. Fournet, A.; Hocquemiller, R.; Roblot, F.; Cavé, A.; Richomme, P.; Bruneton, J. *J. Nat. Prod.* **1993**, *56*, 1547.
13. Fournet, A.; Ferreira, M. E.; Rojas De Arias, A.; Torres De Ortiz, S.; Fuentes, S.; Nakayama, H.; Schinini, A.; Hocquemiller, R. *Antimicrob. Agents Chemother.* **1996**, *40*, 2447.
14. Nakayama, H.; Ferreira, M. E.; Arias, A. R. D.; Bilbao, N. V. D.; Torres, S.; Schinini, A.; Fournet, A. *Phytother. Res.* **2001**, *15*, 630.
15. Fakhfakh, M. A.; Fournet, A.; Prina, E.; Mouscadet, J.-F.; Franck, X.; Hocquemiller, R.; Figadère, B. *Biorg. Med. Chem.* **2003**, *11*, 5013.
16. Ponte-Sucre, A.; Faber, J. H.; Gulder, T.; Kajahn, I.; Pedersen, S. E. H.; Schultheis, M.; Bringmann, G.; Moll, H. *Antimicrob. Agents Chemother.* **2006**, *51*, 188.
17. Bender, A. Databases: Compound bioactivities go public *Nat. Chem. Biol.* **2010**, *6*, 309.
18. Gaulton, A.; Bellis, L.; Chambers, J.; Davies, M.; Hershey, A.; Light, Y.; McGlinchey, S.; Akhtar, R.; Atkinson, F.; Bento, A. P.; Al-Lazikani, B. *Nucleic Acids Res.* **2011**, *40*, D1100.
19. Bolton, E.; Wang, Y.; Thiessen, P. A.; Bryant, S. H. PubChem: Integrated Platform of Small Molecules and Biological Activities In *Annual Reports in Computational Chemistry*; American Chemical Society: Washington, DC, 2008; Vol. 4,.
20. Wang, Y.; Bolton, E.; Dracheva, S.; Karapetyan, K.; Shoemaker, B. A.; Suzek, T. O.; Wang, J.; Xiao, J.; Zhang, J.; Bryant, S. H. *Nucleic Acids Res.* **2010**, *38*, D255.
21. Liu, T.; Lin, Y.; Wen, X.; Jorissen, R. N.; Gilson, M. K. *Nucleic Acids Res.* **2007**, *35*, D198.
22. Hill, J. H. M. *J. Org. Chem.* **1965**, *30*, 620.
23. Brito-Arias, M.; Castillo-Juárez, K.; Molins, E. *Acta Crystallogr., Sect. E: Struct. Rep. Online* **2006**, *62*, o5261.
24. MOE. MOE. Montreal: Chemical Computing Group; 2009.
25. Medina-Franco, J. L.; Martinez-Mayorga, K.; Giulianotti, M. A.; Houghten, R. A.; Pinilla, C. *Curr. Comput.-Aided Drug Des.* **2008**, *4*, 322.
26. Lopez-Vallejo, F.; Peppard, T. L.; Medina-Franco, J. L.; Martinez-Mayorga, K. Computational methods for the discovery of mood disorder therapies *Expert Opin. Drug Discovery* **2011**, *6*, 1227.
27. Medina-Franco, J. L.; Martínez-Mayorga, K.; Bender, A.; Marín, R. M.; Giulianotti, M. A.; Pinilla, C.; Houghten, R. A. *J. Chem. Inf. Model.* **2009**, *49*, 477.
28. OpenEye. OEChem. Santa Fe, NM USA: OpenEye Scientific Software, Inc., http://www.eyesopen.com; 2010.
29. Yongye, A. B.; Bender, A.; Martinez-Mayorga, K. *J. Comput. Aided. Mol. Des.* **2010**, *24*, 675.
30. Hawkins, P. C. D.; Skillman, A. G.; Nicholls, A. *J. Med. Chem.* **2006**, *50*, 74.
31. Sykes, M. J.; McKinnon, R. A.; Miners, J. O. *J. Med. Chem.* **2008**, *51*, 780.
32. Yongye, A. B.; Appel, J. R.; Giulianotti, M. A.; Dooley, C. T.; Medina-Franco, J. L.; Nefzi, A.; Houghten, R. A.; Martinez-Mayorga, K. *Biorg. Med. Chem.* **2009**, *17*, 5583.
33. Martinez-Mayorga, K.; Medina-Franco, J. L.; Giulianotti, M. A.; Pinilla, C.; Dooley, C. T.; Appel, J. R.; Houghten, R. A. *Biorg. Med. Chem.* **2008**, *16*, 5932.
34. Waddell, J.; Medina-Franco, J. L. *Biorg. Med. Chem.*, in press. doi:10.1016/j.bmc.2011.11.051.
35. Yongye, A. B.; Byler, K.; Santos, R.; Martínez-Mayorga, K.; Maggiora, G. M.; Medina-Franco, J. L. *Chem. Inf. Model.* **2011**, *51*, 1259.
36. Brener, Z. *Revista do Instituto de Medicina Tropical de Sao Paolo* **1962**, *4*, 389.
37. Glide. Glide. New York, NY: Schrödinger, LLC; 2010.